Materials Letters 245 (2019) 68–72

Contents lists available at ScienceDirect

Materials Letters

journal homepage: www.elsevier.com/locate/mlblue

Featured Letter

Synergistic effect of a crystal modifier and screw dislocation step defects on the formation mechanism of nickel micro-nanocone

Ehsan Rahimi [a,b], Ali Rafsanjani-Abbasi [a], Amin Imani [c], Ali Reza Kiani Rashid [a], Saman Hosseinpour [d,*], Ali Davoodi [a,*]

[a] Materials and Metallurgical Engineering Department, Faculty of Engineering, Ferdowsi University of Mashhad, Mashhad 9177948974, Iran
[b] Department of Engineering and Architecture, University of Udine, Via Cotonificio 108, 33100 Udine, Italy
[c] Department of Materials Engineering, University of British Columbia, Vancouver, BC V6T 1Z4, Canada
[d] Institute of Particle Technology (LFG), Friedrich-Alexander-Universität-Erlangen-Nürnberg (FAU), Cauerstraße 4, 91058 Erlangen, Germany

ARTICLE INFO

Article history:
Received 11 February 2019
Received in revised form 22 February 2019
Accepted 23 February 2019
Available online 26 February 2019

Keywords:
Screw dislocation
Step edge
Crystal modifier
DFT and Monte Carlo simulations

ABSTRACT

The synergestic role of boric acid, as a crystal modifier, and screw dislocation step defects on the crystal growth and formation mechanism of nickel micro-nanocones during electrocrystallization is explained using density functional theory (DFT) and Monte Carlo (MC) calculations. Earlier atomic force microscopy (AFM) studies provided direct evidences on the effect of boric acid on morphology distribution of nickel micro-nanocones and confirmed the presence of terraces and steps due to the spiral growth of screw dislocation. In the presence of boric acid, the formation of nickel-borate complex leads to a decrease in the system's supersaturation and in turn provides an appropriate condition for screw dislocation driven-growth. DFT and MC simulations reveal that the nickel-borate complex primarily adsorb in the step edges with the lowest adsorption energy barrier, after which the crystal growth is inhibited on these edges resulting in the formation of nanocone structures.

1. Introduction

Understanding the crystals growth mechanisms is a crucial step towards controlling the shape, size, and functionality of the complex crystalline structures in modern materials [1–8]. Dislocation-driven nanostructure formation, especially from screw dislocation defects, plays a key role in the growth of almost all crystals relevant for energy storage, catalysis, and nanoelectronic applications [9,22]. This type of growth mechanisms is dominated in systems with the low supersaturation where screw dislocations often intersect with the surface and create step edges which permit the continuous spiral crystal growth [10,11].

During the electrocrystallization process supersaturation of the system is the main driving force for crystal growth [11]. This driving force is directly affected by the applied current density [12,23] and by the presence of crystal modifiers. Previous studies show that boric acid (H_3BO_3), as a crystal modifier, decreases the supersaturation and increases the current efficiency during the formation of micro or nanostructures in an electrodeposition process [13–15].

The step edge of screw dislocation is a prominent location, with the lowest energy barrier, for nucleate and growth of ions or complexes [11]. Therefore, determining the motif in which the crystal modifier molecules adsorb on these sites and subsequently the synergistic mechanism of which the screw dislocation crystal growth leads to the formation of three-dimensional micro- or nanostructures are of great importance. Boric acid is known to form complex with metal ions, which plays a significant role in the crystal growth mechanism, as reported in previous studies [13,16,17]. In the present work, we used the density functional theory (DFT), molecular dynamics (MD) simulation, to investigate the adsorption mechanism of nickel-borate complex on screw dislocation step edges of the Ni and its effect on the formation of the three-dimensional micro-nanostructure, which was observed experimentally in our previous atomic force microscopy (AFM) studies [18].

2. Experimental procedure

2.1. Material and electrodeposition method

The materials and electrodeposition conditions as well as microstructural and chemical analysis using scanning electron

* Corresponding authors.
E-mail addresses: saman.hosseinpour@fau.de (S. Hosseinpour), a.davodi@um.ac.ir (A. Davodi).

https://doi.org/10.1016/j.matlet.2019.02.093
0167-577X/

microscopy (SEM), X-ray diffraction (XRD) and AFM are discussed in our previous work [18].

2.2. Simulation analysis

The quantum chemical calculation of the nickel-borate complex was carried out by DMol3 based on DFT in Materials Studio (V. 8.0 Accelrys Inc. software). The functional of Becke exchange plus Lee–Yang–Parr correlation (BLYP) was selected in order to calculate the quantum chemical parameters of a nickel-borate molecule. These parameters include the geometrical optimization, the total electrostatic potential, the highest occupied molecular orbital (HOMO), and the lowest unoccupied molecular orbital (LUMO). Additionally, partial density of states (PDOSs) were calculated by the Monkhorst-Pack k-point grid for a quick visual analysis of the electronic structure of the nickel-borate molecule.

To investigate the adsorption mechanism of nickel-borate molecule different surfaces, i.e. Cu (1 0 0), Ni (1 1 1), and Ni (2 2 0) with simple and screw dislocation step edges were chosen as substrates. Monte Carlo (MC) simulation was performed using the adsorption locator module and COMPASS force field.

3. Results and discussion

To investigate the characteristic electronic structure of the nickel-borate complex, we calculated the PDOSs alongside the most important quantum chemical parameters such as the HOMO, LUMO, the band gap energy ($\Delta E = E_{HOMO} - E_{LUMO}$), and electrostatic potential. In Fig. 1a the optimized geometry of nickel-borate complex, HOMO and LUMO as well as the distribution of electrostatic potentials are depicted. Possible effects of external fields on the stability or optimized geometry of the nickel-borate complex are not considered in our calculations. Based on DFT and frontier molecular orbital theory calculation results HOMO and LUMO energy values of the nickel-borate molecule are −7.19 eV and −3.83 eV, respectively. The band gap energy for the nickel-borate molecule is thus 3.36 eV. Fig. 1b shows the PDOSs for the nickel-borate molecule below and above the Fermi level (E_F). The PDOSs analysis provides a deeper insight on the interaction of the nickel-borate molecule with different surfaces based on its electron density distribution. In this figure a larger fraction of occupied orbitals are observed in the left part of (E_F) (occupied states) compare to that in the right part of E_F (unoccupied states) [19]. Furthermore, the occupied states for all orbitals of the nickel-borate complex are much closer to E_F in comparison with unoccupied states. E_F indeed lies in the valance band with the main contribution of p and s electrons states. According to PDOS analysis and considering the HOMO energy value, the nickel-borate complex has a high tendency to donate electrons to an appropriate acceptor (in this study Cu and Ni surfaces) before and during the electrocrystallization process.

Screw dislocation step edges are expected to play an important role during reduction of nickel ions and nickel-borate complexes, by reducing the adsorption energy barrier. The step edges provide low energy migration paths for molecular junctions of these species. To reveal the synergistic effect of screw dislocation step edges on the adsorption mechanism of nickel-borate complex during the electrocrystallization process we performed MC simulations on Cu and Ni plane surfaces with different step structures.

Fig. 2 shows the adsorption configuration of a single nickel-borate molecule on Cu (1 0 0) plane with the flat surface condition in the aqueous medium including 100 water molecules. As we demonstrated earlier, the competitive adsorption of water molecules and organic adsorbates may highly influence the final adsorption configuration [20]. The slide and top view images (Fig. 2a) demonstrate that the nickel-borate molecule adopts a flat configuration on Cu (1 0 0), with mean distance of ~9 Å from the surface. In comparison, the nickel-borate complex after adsorption on Ni (1 1 1) adopts a shorter distance (mean distance value ~5 Å). The closer distance of the nickel-borate molecule to Ni surface than that on Cu is related to the electronic property of Ni having a higher work function in comparison to Cu [21]. Likewise, the mean adsorption energy for the nickel-borate complex on Ni (1 1 1) (−1927.4 kcal.mol^{-1}) is slightly lower than that on Cu (1 0 0) (−1918.1 kcal.mol^{-1}). Fig. 2c and d, on the other hand, show that simple and screw dislocation step edges on Ni (2 2 0) plane also provide suitable sites for adsorption of the nickel-borate complex. However, the adsorption geometry of nickel-borate complex on these step edges is different from those on terraces. The adsorption configuration of the molecule on the step edge is almost perpendicular to the edge and very close to it (with a distance of ~3.4 Å). The step edges provide adsorption sites with lower energy barrier compared to terraces. Similarly, nucleation and growth mechanism on these edges is facilitated during the spiral screw formation in the low supersaturation. According to MC simulation results in Fig. 2d, the adsorbed nickel-borate complexes on screw dislocation adopt two configurations with the lowest adsorption energy barrier, with perpendicular and flat configurations.

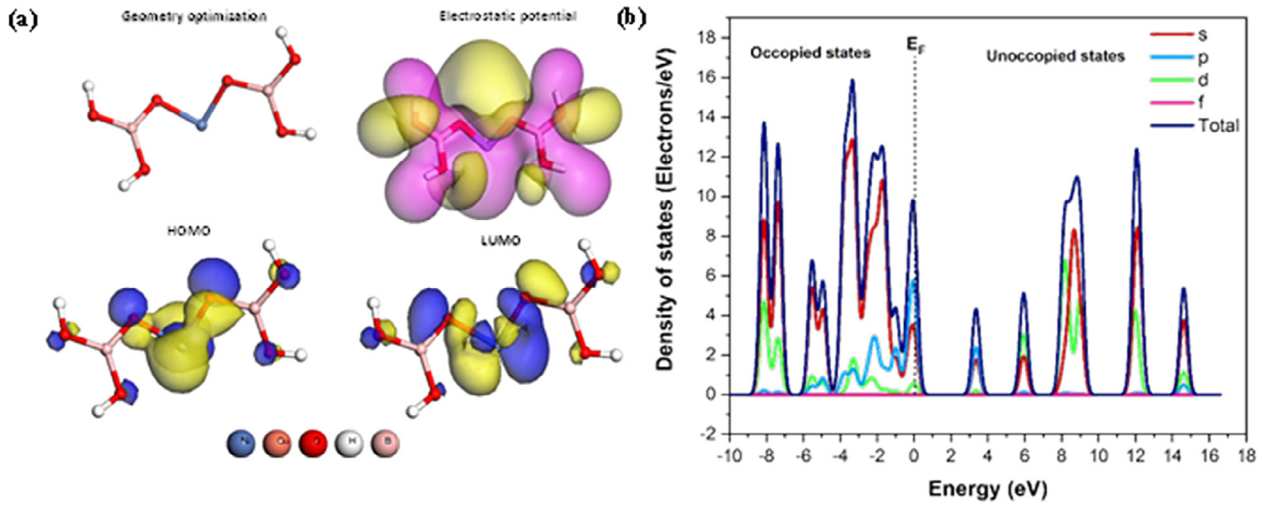

Fig. 1. (a) The quantum chemical calculations of the nickel-borate molecule, (b) The partial density of states (PDOS) analysis of nickel-borate molecule based on DMol3 calculations.

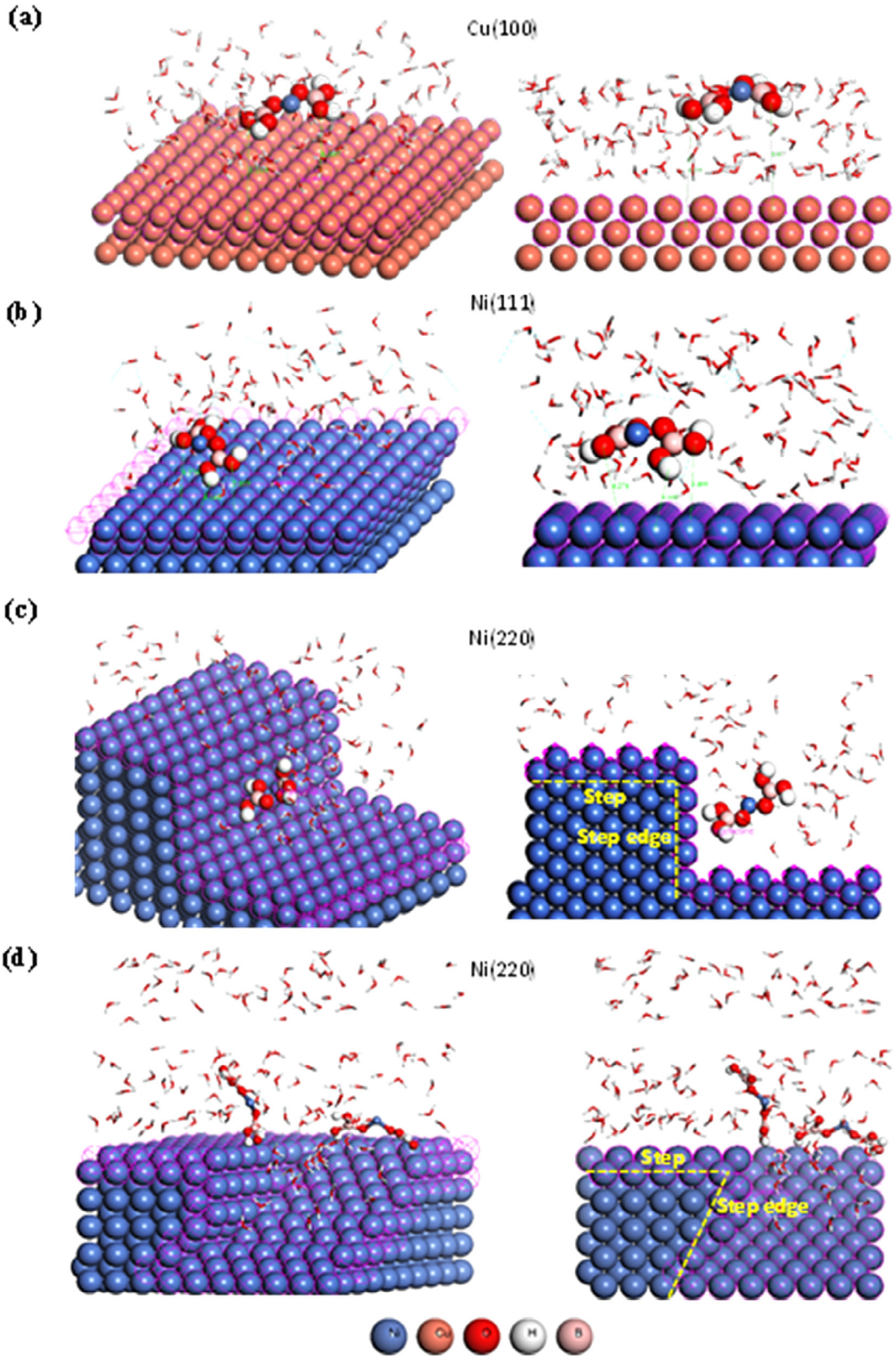

Fig. 2. Top and slide views of nickel-borate molecule adsorption configuration in the presence of 100 water molecule during electrocrystallization process on (a) Cu (1 0 0) with supercell 24 × 24 × 15 Å, (b) Ni (1 1 1) with supercell 24 × 24 × 14 Å, (c) Ni (2 2 0) with simple step edge and supercell 33 × 22 × 15 Å, and (d) Ni (2 2 0) with screw dislocation step edge with supercell 33 × 22 × 11 Å.

According to MC calculation, the mean value of adsorption energy for nickel-borate complex on step edge of screw dislocation (-2769.9 kcal.mol^{-1}) is significantly lower than that on simple step edge (-2591.5 kcal.mol^{-1}). Therefore, screw dislocation step edge is the most favorable adsorption site for nickel-borate complex. Occupation of the (2 2 0) plane of the step edge of screw

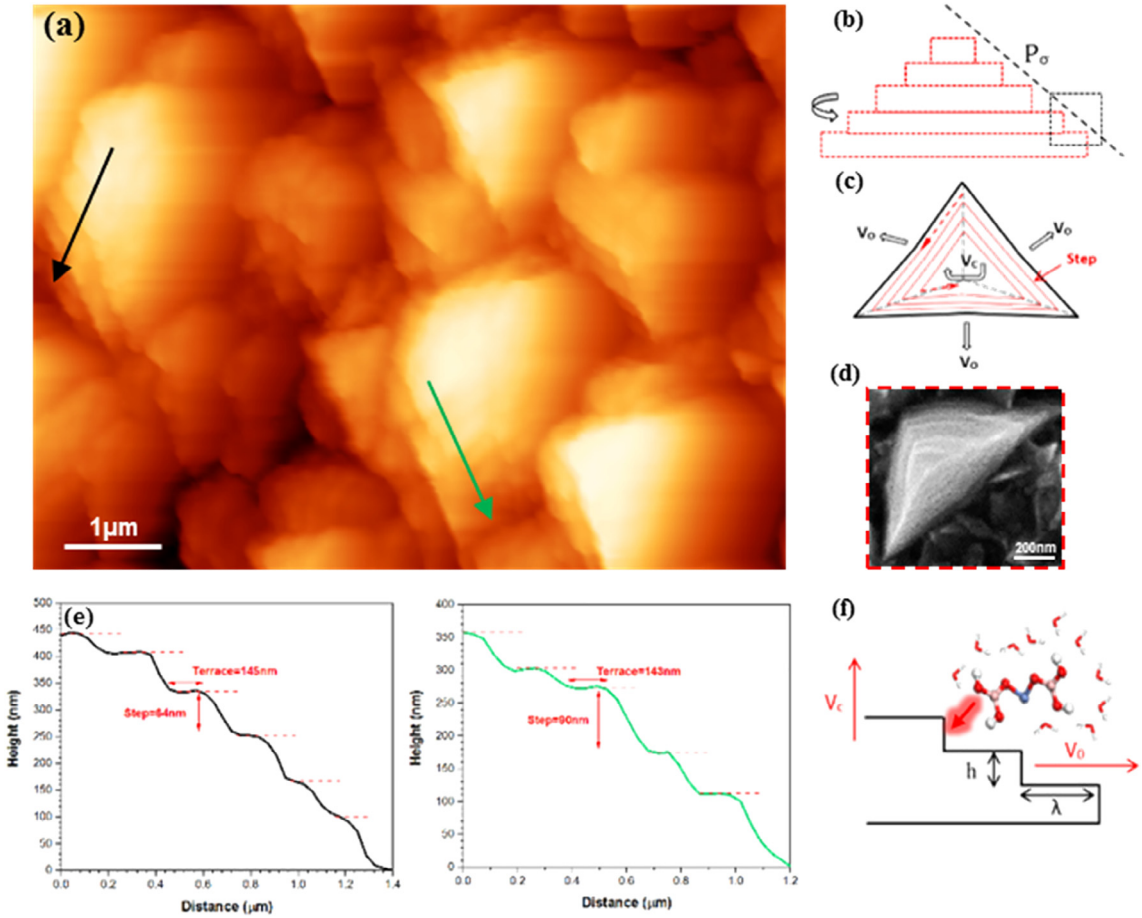

Fig. 3. (a, e) AFM image and line profiles of nickel micro-nanocones, (b, c) Top and slide views schematically images of screw dislocation propagation with different velocities, (d) SEM image of single nickel microcone, (f) schematically demonstration of nickel-borate molecule adsorption effect on crystal growth velocities, step height, and terrace width of microcone.

dislocation by surface bond nickel-borate complex, however, changes the preferred growth orientation of the crystal from (2 2 0) to (2 0 0) facet. Consequently, the synergistic effect of the presence of screw dislocation step edge and nickel-borate complex adsorbate facilitates the conditions for formation of hierarchical nickel micro-nanostructures, as shown in Fig. 3.

The topography line profiles in Fig. 3e confirm the formation of terraces and step heights during the electrocrystallization process, which have been created by screw dislocation-driven growth. The slide and top view images in Fig. 3b and c schematically depict the orientations of the crystal growth originated from a screw dislocation, specifying the velocity of steps at the core (V_c) and outer edges of the dislocation (V_o) (definition can be found in Ref. [7]). In the presence of boric acid, growth in V_o direction is inhibited due to the capping effect of boric acid and crystal growth occurs predominantly in V_c direction, as shown in Fig. 3f. This increase of growth in V_c direction is in a good agreement with the PSD analysis of the experimental AFM results [18], demonstrating the formation of nanostructures during electrocrystallization in the presence of boric acid.

4. Conclusions

Density functional theory (DFT) simulation and Monte Carlo (MC) calculation were performed to explain the synergistic behavior between boric acid, as a crystal modifier, and screw dislocation step edge in the crystal growth of electrodeposited Ni films on Cu. MC calculations showed that step edges of screw dislocations on Ni surface are preferred adsorption location for nickel-borate complex, with the lowest adsorption energy barrier compared to simple step edges and flat nickel terraces. Nevertheless, after adsorption, the capping effect of boric acid results in an inhibition of the crystal growth in Ni (2 2 0) plane direction while promoting the growth along Ni (2 0 0) plane direction. Such controlled growth mechanism, driven by a low supersaturation during electrocrystallization, in turn results in formation of a micro- and nanocone-like morphology, in agreement with the experimental AFM results.

Conflict of interest

None.

Acknowledgments

Ferdowsi University of Mashhad and Hakim Sabzevari University are appreciated for providing simulation and experimental setups.

References

[1] Y. Deng, H. Ling, X. Feng, et al., CrystEngComm 17 (2015) 868–876.
[2] T. Hang, M. Li, Q. Fei, et al., Nanotechnology 19 (2008) 35201.
[3] W. Zhang, Z. Yu, Z. Chen, et al., Mater. Lett. 67 (2012) 327–330.
[4] Zhihui Cai, Yong Liu, Yang Song, et al., J. Cryst. Growth 461 (2017) 1–9.
[5] F. Meng, S.A. Morin, A. Forticaux, et al., Acc. Chem. Res. 46 (2013) 1616–1626.
[6] M.W. Anderson, J.T. Gebbie-Rayet, A.R. Hill, et al., Nature 544 (2017) 456.

[7] S.A. Morin, A. Forticaux, M.J. Bierman, et al., Nano Lett. 11 (2011) 4449–4455.
[8] A. Majumder, Z.K. Nagy, Chem. Eng. Sci. 101 (2013) 593–602.
[9] J.N. Clark, J. Ihli, A.S. Schenk, et al., Nat .Mater. 14 (2015) 780–784.
[10] W. Obretenov, J. Electrochem. Soc. 140 (1993) 692.
[11] E. Budevski, G. Staikov, W.J. Lorenz, Electrochim. Acta 45 (2000) 2559–2574.
[12] J.M. Lee, K.K. Jung, J.S. Ko, Curr. Appl. Phys. 16 (2016) 261–266.
[13] L.M. Graham, S. Cho, S.K. Kim, et al., Chem. Commun. (Camb) 50 (2014) 527–529.
[14] M. Šupicová, R. Rozik, L. Trnková, et al., J. Solid State Electr. 10 (2006) 61–68.
[15] J.M. Lee, K.K. Jung, J.S. Ko, J. Electrochem. Soc. 163 (2016) D407–D413.
[16] E.-B. Cho, M. Mandal, M. Jaroniec, Chem. Mater. 23 (2011) 1971–1976.
[17] E. Rahimi, A. Rafsanjani-Abbasi, A. Kiani-Rashid, et al., Colloids Surfaces A 547 (2018) 81–94.
[18] E. Rahimi, A. Davoodi, A.R. Kiani Rashid, Mater. Lett. 210 (2018) 341–344.
[19] C.E. Lekka, G.A. Evangelakis, Scripta Mater. 61 (2009) 974–977.
[20] E. Naseri, M. Hajisafari, A. Kosari, et al., J. Mol. Liq. 269 (2018) 193–202.
[21] H.B. Michaelson, J. Appl. Phys. 48 (1977) 4729–4733.
[22] S. Jin, M.J. Bierman, S.A. Morin, J. Phys. Chem. Lett. 1 (9) (2010) 1472–1480, https://doi.org/10.1021/jz100288z.
[23] S.I. Ghazanlou, A.H.S. Farhood, S. Ahmadiyeh, E. Ziyaei, A. Rasooli, S. Hosseinpour, Metallur. Mater. Trans. A 50 (4) (2019) 1922–1935, https://doi.org/10.1007/s11661-019-05118-y.